Downregulation of CUEDC2 prevents doxorubicin-induced cardiotoxicity in H9c2 cells

XIANPU ZHANG, JIAOJIAO LI, YONGBO CHENG, JIANGUANG YI, XIN LIU and WEI CHENG

Department of Cardio-Thoracic Surgery, Southwest Hospital,
The First Affiliated Hospital of Third Military Medical University (Army Medical University), Chongqing 400038, P.R. China

Received October 4, 2017; Accepted February 16, 2018

DOI: 10.3892/mmr.2018.9072

Abstract. Treatment with doxorubicin (DOX), which is an effective anticancer agent, is limited by cardiotoxicity. CUE domain-containing 2 (CUEDC2) serves a role in numerous cellular processes. The present study aimed to elucidate the potential function of CUEDC2 in DOX-induced cardiotoxicity. Cell Counting kit-8 assay demonstrated that DOX induced cytotoxicity of H9c2 cells in a dose-dependent manner. Flow cytometry demonstrated that downregulation of CUEDC2 reduced the levels of DOX-induced reactive oxygen species. Furthermore, compared with in the DOX-treated group, the activity of superoxide dismutase was increased in the DOX + small interfering RNA (si)CUEDC2 group; whereas, the malondialdehyde content was reduced in the DOX + siCUEDC2 group. In addition, flow cytometric analysis indicated that mitochondrial membrane potential was maintained following the depletion of CUEDC2. Furthermore, CUEDC2 downregulation significantly inhibited DOX-induced apoptosis. The expression levels of proapoptotic genes, including B-cell lymphoma 2 (Bcl-2)-associated X protein, cleaved caspase-3 and cytochrome *c* were inhibited by the depletion of CUEDC2. Conversely, the expression levels of the anti-apoptotic gene Bcl-2 were elevated in the CUEDC2 knockdown group. Downregulation of CUEDC2 also increased phosphorylation of protein kinase B and forkhead box O3a, and decreased the expression of Bcl-2-like protein 11 according to western blot analysis. Taken together, the present study demonstrated that CUEDC2 downregulation prevented DOX-induced cardiotoxicity in H9c2 cells. Therefore, CUEDC2 may be a promising target for the prevention of DOX-induced cardiotoxicity.

Correspondence to: Dr Wei Cheng, Department of Cardio-Thoracic Surgery, Southwest Hospital, The First Affiliated Hospital of Third Military Medical University (Army Medical University), 29 Main Street, Chongqing 400038, P.R. China
E-mail: weichengouu@163.com

Key words: CUE domain-containing 2, doxorubicin, cardiotoxicity, protein kinase B/forkhead box O3/Bcl-2-like protein 11

Introduction

Doxorubicin (DOX) is a broad-spectrum anthracycline antibiotic, which can interact with topoisomerase II complex, thereby inhibiting the progression of DNA replication (1,2); therefore, DOX is often used to treat solid tumors and certain types of leukemia. However, its clinical use is limited by side effects, including vomiting, hair loss, inflammation and heart injury (3). Among these side effects, cardiomyopathy is the most severe and is caused by increased generation of reactive oxygen species (ROS) (4,5). Mitochondria serve a central role in production of intracellular energy and are the primary target of DOX-induced toxicity (6). Once mitochondrial dysfunction occurs, apoptosis or programmed cell death is activated. It has previously been reported that DOX can induce apoptosis by arresting cell cycle progression (7). DOX-induced ROS release is mediated by signaling pathways and triggers apoptosis of myocardial cells. Protein kinase B (AKT) is a serine/threonine kinase, which serves a role in various biological events, including cell survival, apoptosis and metabolism. In addition, forkhead box protein O (FOXO) transcription factors modulate apoptosis and resistance to oxidative stress (8). Activated AKT via phosphorylation regulates its downstream targets via kinase activity. It has been reported that FOXO3a is a member of the FOXO protein family, which can be phosphorylated by this activated signal (9). Phosphorylation of FOXO3a may lead to its nuclear export and suppression of the transcription of its target genes. Conversely, apoptotic signals may result in dephosphorylation of FOXO3a and therefore activate the expression of its target genes (10-12). It has previously been revealed that B-cell lymphoma 2 (Bcl-2)-like protein 11 (Bim) has an important role in the underlying mechanisms associated with programmed death and stress-mediated apoptosis, which can be regulated by FOXO3a. Furthermore, inhibition of AKT activity has been demonstrated to enhance the expression levels of Bim (12). Based on these findings, prevention of apoptosis may be a potential treatment strategy for DOX-induced cardiotoxicity.

CUE domain-containing 2 (CUEDC2) is extensively expressed in the brain, testes and heart; it has previously been reported that CUEDC2 promotes ubiquitination and degradation of progesterone receptors (13). CUEDC2 is associated with the cell cycle and inflammation (14), and it has been revealed to be abnormally expressed in tumors, including kidney,

brain, ovarian and breast cancer (14). However, the potential function of CUEDC2 in DOX-induced cardiotoxicity remains to be completely elucidated. The present study focused on determining the effects of CUEDC2 on DOX-induced cardiotoxicity and elucidating the underlying molecular mechanism.

In the present study, downregulation of CUEDC2 alleviated DOX-induced cardiotoxicity by reducing oxidative stress and suppressing apoptosis. Furthermore, it was demonstrated that this attenuated cardiotoxicity may be caused by the phosphorylation of AKT/FOXO3a and decreased expression of Bim. The results indicated that CUEDC2 may be considered a promising target in the prevention of DOX-induced cardiotoxicity.

Materials and methods

Cell culture and treatment groups. The H9c2 cell line (American Type Culture Collection, Manassas, VA, USA) was grown at 37˚C in Dulbecco's modified Eagle's medium (DMEM; Gibco; Thermo Fisher Scientific, Inc., Waltham, MA, USA) containing 10% fetal bovine serum (Sigma-Aldrich; Merck KGaA, Darmstadt, Germany) and 10% penicillin/streptomycin in an atmosphere containing 5% CO_2. The phenotype of myocardial cells was initially observed under a light microscope (magnification, x40). The negative small interfering (si) RNA scramble control (siSCR), CUEDC2 siRNA (siCUE) and reverse transcription-quantitative polymerase chain reaction (RT-qPCR) primers were purchased from Santa Cruz Biotechnology, Inc. (Dallas, TX, USA). At ~80% confluence, cells were divided into the following groups: i) untreated cells (control); ii) cells transfected with siSCR; iii) cells treated with 1 μM DOX (Sigma-Aldrich; Merck KGaA) at 37˚C for 24 h (DOX); iv) cells transfected with siSCR and treated with 1 μM DOX at 37˚C for 24 h (DOX + siSCR); and v) cells transfected with siCUE and treated with 1 μM DOX at 37˚C for 24 h (DOX + siCUE). All experiments were carried out independently at least three times.

Cell transfection. According to the manufacturer's protocol, cells ($1x10^5$) were seeded into 6-well plates and maintained in serum-free medium overnight. Briefly, Lipofectamine® 2000 (Invitrogen; Thermo Fisher Scientific, Inc., Waltham, MA, USA) was mixed with serum-free DMEM. After 5 min, the resulting regent was divided into three centrifuge tubes, containing: i) 10 μl Lipofectamine® 2000 alone, ii) 10 μM siScr (cat. no. sc-37007; Santa Cruz Biotechnology, Inc.) or iii) 10 μM siCUE (cat. no. sc-90791; Santa Cruz Biotechnology, Inc.), according to the experimental design. The mixtures were incubated at room temperature for 20 min. Subsequently, the liposome mixtures were added to the cells. After a 6 h incubation at 37˚C, the transfection medium was removed and supplemented with normal culture medium or DOX for 1 h. The cells were collected a total of 24 h post-transfection and then subjected to subsequent assays.

Cell Counting kit-8 (CCK-8) assay. The CCK-8 method was used to determine cell viability. Briefly, cells ($1x10^5$) were seeded in 96-well plates and treated with DOX (0.1, 0.5, 1 and 5 μM) for 24, 36 and 48 h time intervals. The collected cells were then treated with CCK-8 solution (10 μl; cat. no. C0038; Beyotime Institute of Biotechnology, Haimen, China) for 4 h at 37˚C. The absorbance was measured at a wavelength of 450 nm using a microplate reader (Promega Corporation, Madison, WI, USA).

Flow cytometric analysis of ROS. Cells were stained with the oxidant-sensitive fluorescent probe 2',7'-dichlorodihydrofluorescein diacetate (DCFH-DA; cat. no. 35845; Sigma-Aldrich; Merck KGaA) for 15 min and were washed with PBS. 2',7'-Dichlorofluorescein (DCF) was generated from DCFH-DA in the presence of peroxide. The fluorescence of DCF was detected using Accuri C6 flow cytometry (BD Biosciences, Franklin Lakes, NJ, USA) with an excitation wavelength of 485 nm. Data analysis was performed using Accuri CFlow Plus software (version 1.0; BD Biosciences).

Mitochondrial membrane potential (MMP) determination. The JC-1 probe can emit green fluorescence at low membrane potentials and red fluorescence at increased potentials. MitoProbe™ JC-1 Assay kit (cat. no. M34152; Invitrogen; Thermo Fisher Scientific, Inc.) was used to determine MMP, according to the manufacturer's protocol. Briefly, the cells were stained with JC-1 for 20 min at 37˚C and were then loaded onto an Accuri C6 flow cytometer (BD Biosciences). The ratio of red/green fluorescence was calculated and a decrease in the ratio indicated loss of MMP. Data analysis was performed with Accuri CFlow Plus software (version 1.0; BD Biosciences).

Flow cytometric analysis of apoptosis. The Annexin V-fluorescein isothiocyanate (FITC)/propidium iodide (PI) kit (cat. no. V13241; Invitrogen; Thermo Fisher Scientific, Inc.) was used to detect apoptosis. Annexin V-$FITC^+/PI^-$ indicated early apoptotic cells, whereas late apoptotic cells were represented as Annexin V-$FITC^+/PI^+$. According to the manufacturer's protocol, following treatment, cells in a 24-well plate ($1x10^5$ cells/well) were stained with Annexin V-FITC and PI for 10 min at room temperature in the dark, after which fluorescence intensity was analyzed using Accuri C6 flow cytometry with Accuri CFlow Plus software version 1.0 (BD Biosciences).

Activity measurement of oxidative indicators. Superoxide dismutase (SOD; cat. no. S0101), catalase (CAT; cat. no. S0051) and malondialdehyde (MDA; cat no. S0131) were spectrophotometrically determined in collected cells following treatment using commercial assay kits, according to the manufacturer's protocols (Beyotime Institute of Biotechnology). SOD and CAT activity was presented as units per mg of protein, and MDA content was presented as nmol/mg.

RNA isolation and RT-qPCR. Total RNA was isolated from the cells using TRIzol® regent (Invitrogen; Thermo Fisher Scientific, Inc). cDNA was synthesized from 2 μg RNA using oligo-dT primers (New England BioLabs, Inc., Ipswich, MA, USA) and M-MLV reverse transcriptase (Promega Corporation), according to manufacturer's protocol. qPCR was conducted on the Mastercycler® ep realplex system (Eppendorf, Hamburg, Germany) using SYBR Green PCR master mix (Takara Bio, Inc., Otsu, Japan), according to the manufacturer's protocol. The thermocycling conditions

used for qPCR were as follows: 95˚C for 5 min; followed by 36 cycles of 95˚C for 30 sec and 60˚C for 30 sec; followed by 72˚C for 7 min. The relative expression levels of target genes were normalized to the expression of the housekeeping gene GAPDH. The following primer sequences were used for qPCR: Bcl-2-associated X protein (Bax), forward 5'-TGG CCTCCTTTCCTACTTCG-3', reverse 5'-AAAATGCCTTTC CCCGTTCC-3'; Bcl-2, forward 5'-CACACACACACATTC AGGCA-3', reverse 5'-GGCAATTCCTGGTTCGGTTT-3'; caspase-3, forward 5'-CTCGCGTTAACAGGAAGGTG-3', reverse 5'-GGCAGTGGTAGCGTACAAAG-3'; cytochrome *c*, forward 5'-AGAGTGAGTTCCAGGACAGC-3', reverse 5'-ACTAACGAGGCCCCTTTGAA-3'; and GAPDH, forward 5'-GGGTCCCAGCTTAGGTTCAT-3' and reverse 5'-CAT TCTCGGCCTTGACTGTG-3'. Quantification of RT-qPCR products was performed using the $2^{-\Delta\Delta Cq}$ method (15).

Western blot analysis. Total proteins were extracted using radioimmunoprecipitation assay (Beijing Solarbio Science & Technology, Co., Ltd., Beijing, China) and were boiled. A BCA protein quantification kit (Bio-Rad Laboratories, Inc., Hercules, CA, USA) was used to determine the protein concentration. Subsequently, protein samples from each group (20 μg) were separated by 10% SDS-PAGE and transferred onto PVDF membrane. Following blocking with fat-free milk for 2 h at room temperature, the membrane was incubated with primary antibodies overnight at 4˚C. Prior to incubation with secondary antibodies at room temperature for 1 h, the membrane was washed with Tris-buffered saline containing 0.1% Tween. Protein bands were visualized using BeyoECL Plus reagent (Beyotime Institute of Biotechnology). The following antibodies were used for western blotting: Anti-phosphorylated (p)-FOXO3a (cat. no. ab53287; 1:1,000), anti-Bcl-2 (cat. no. ab59348; 1:700) and anti-Bax (cat. no. ab53154; 1:1,000) from Abcam (Cambridge, UK); anti-CUEDC2 (cat. no. 12294; 1:1,000), anti-FOXO3a (cat. no. 2497; 1:1,000), anti-cytochrome *c* (cat. no. 11940; 1:1,000), anti-cleaved caspase-3 (cat. no. 9664; 1:1,000), anti-p-AKT (Thr308; cat. no. 13038; 1:1,000), anti-AKT (cat. no. 4691; 1:1,000), anti-Bim (cat. no. 2819; 1:1,000) and anti-GAPDH (cat. no. 5174; 1:1,000) from Cell Signaling Technology, Inc. (Danvers, MA, USA). Horseradish peroxidase-conjugated goat anti-rabbit secondary antibody (cat. no. sc-2004; 1:5,000) was supplied by Santa Cruz Biotechnology, Inc. Denistometric analysis was performed using Quantity One software (version 4.6.2; Bio-Rad Laboratories, Inc.).

Statistical analysis. Statistical analyses were performed using GraphPad Prism (version 6.0; GraphPad Software, Inc., La Jolla, CA, USA). The difference between groups was analyzed using one-way analysis of variance followed by Dunnett's or Turkey's post hoc tests when appropriate. Data are presented as the means ± standard deviation. $P<0.05$ was considered to indicate a statistically significant difference.

Results

Cytotoxicity of DOX in H9c2 cells. The phenotype of myocardial cells are presented in Fig. 1A and B. Subsequently, cytotoxicity of DOX (0.1, 0.5, 1 and 5 μM) was determined in H9c2 cells. The results of CCK-8 assay demonstrated that viability of H9c2 cells was significantly decreased following incubation with 0.5 μM DOX for 24 h. Cytotoxicity of DOX increased in a dose-dependent manner (Fig. 1C). According to the results presented in Fig. 1C and a previous study (16), 1 μM DOX was selected to establish the cardiotoxicity model in the present study.

Effects of depletion of CUEDC2 on DOX-induced oxidative stress. CUEDC2 is extensively expressed in the heart, and it has been reported that this protein is involved in modulation of the oxidative capacity of cardiomyocytes (17). Therefore, the potential function of CUEDC2 in cardiomyocytes was investigated in subsequent experiments. Following transfection with siRNA, the mRNA and protein expression levels of CUEDC2 were downregulated, thus indicating that knockdown of CUEDC2 was effective (Fig. 1D-F). Formation of ROS has previously been implicated in DOX-induced cardiotoxicity (17). Flow cytometric analysis demonstrated that the levels of ROS were elevated in the DOX group, whereas they were decreased in the DOX + siCUE group (Fig. 2A and B). Intracellular redox homeostasis is dependent on the generation and removal of ROS. Production of MDA and the activity of antioxidative enzymes, including SOD and CAT, can be used to monitor this redox state (18). The results of the present study revealed that DOX markedly increased the content of MDA, whereas depletion of CUEDC2 resulted in a significant decrease in MDA levels. In addition, DOX-reduced SOD activity was rescued by the depletion of CUEDC2, whereas the alterations in CAT activity were not significantly different in the DOX + siCUE group compared with in the DOX group (Fig. 2C).

Effects of CUEDC2 knockdown on MMP. Mitochondria are the primary target organelles of DOX-induced cardiotoxicity (19,20). MMP is necessary for the production of ATP, which serves crucial roles in living cells (21). The results of flow cytometry revealed that DOX induced MMP loss; however, MMP was recovered by the knockdown of CUEDC2 (Fig. 3A and B)

Effects of CUEDC2 knockdown on DOX-mediated apoptosis. Mitochondrial dysfunction is closely associated with apoptosis (22); therefore, the levels of apoptosis were determined in the present study. The results of flow cytometry demonstrated that the rate of apoptosis was lower in the DOX + siCUE group compared with in the DOX group (Fig. 4A and B). The expression levels of apoptosis-associated genes were also detected in the present study. The mRNA expression levels of Bax, caspase-3 and cytochrome *c* were decreased in the DOX + siCUE group compared with in the DOX group (Fig. 5). Conversely, Bcl-2 expression was increased following depletion of CUEDC2. In addition, the protein expression levels of Bax, cleaved-caspase-3 and cytochrome *c* were lower in the DOX + siCUE group compared with in the DOX group, whereas Bcl-2 expression was elevated in the DOX + siCUE group compared with in the DOX group.

Effects of CUEDC2 depletion on the AKT/FOXO3a/Bim signaling pathway. FOXO3a, as a member of the FOXO family

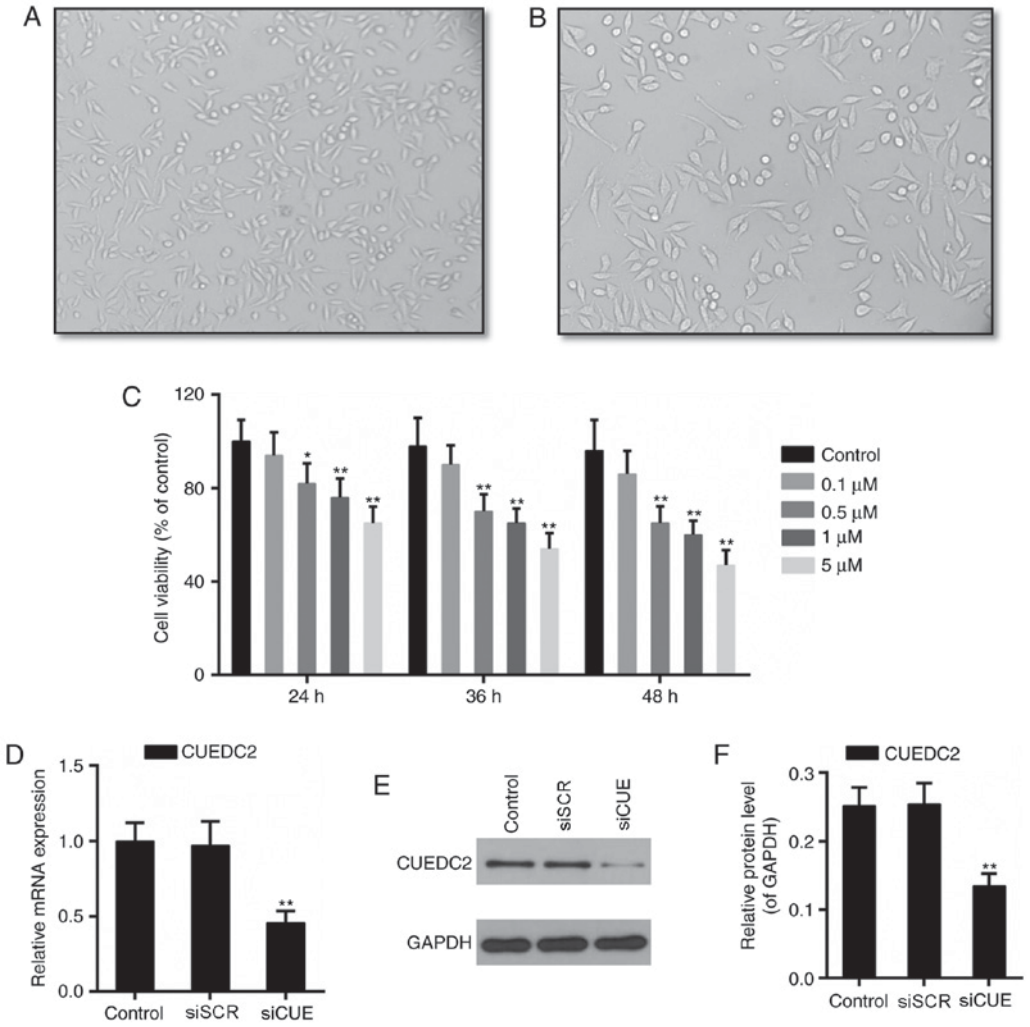

Figure 1. Observation of H9c2 cells under a light microscope: (A) x100 and (B) x200 magnification. (C) Cell Counting kit-8 assay was used to detect DOX-induced cytotoxicity. DOX was administered at a concentration of 0.1, 0.5, 1 and 5 μM. Effects of CUEDC2 siRNA on (D) mRNA and (E) protein expression were determined. (F) Western blot was semi-quantitatively analyzed. *P<0.05 and **P<0.01 vs. the control group. CUEDC2, CUE domain-containing 2; DOX, doxorubicin; siCUE, CUEDC2 siRNA; siRNA, small interfering RNA; siSCR, siRNA scramble control.

of transcription factors, serves a role in the oxidative stress response. It has previously been reported that AKT signaling regulates the activity FOXO3a, which in turn modulates the expression of Bim (23,24). Levels of phosphorylated AKT and phosphorylated FOXO3a were significantly enhanced in the DOX + siCUE group compared with in the DOX group (Fig. 6). Conversely, the elevated protein expression of Bim following treatment with DOX was decreased following depletion of CUEDC2. These findings suggested that siCUE activated phosphorylated AKT, which subsequently phosphorylated FOXO3a and decreased Bim transcription.

Discussion

Despite its high anticancer efficacy, the clinical use of DOX is limited by its acute or cumulative cardiotoxicity (25). CUEDC2 is considered to serve a role in various cellular processes and is abundant in the heart (14); however, little is known about the potential function of CUEDC2 in DOX-induced cardiotoxicity. Therefore, the present study aimed to investigate its function and associated mechanisms. H9c2 cells, which were originally derived from embryonic rat ventricular tissue, can accurately model the response of primary cardiomyocytes (26). As opposed to non-proliferating primary cardiomyocytes, H9c2 cells are able to proliferate (27-29). Therefore, the present study used H9c2 as an *in vitro* model for subsequent experiments.

In the present study, treatment with DOX decreased viability of myocardial cells in a dose-dependent manner. Production of ROS is reported as one of the mechanisms mediating DOX-induced cardiotoxicity (25). The results of the present study demonstrated that depletion of CUEDC2 decreased ROS levels, which were elevated following treatment with DOX. Furthermore, oxidative stress indicators were modulated by depletion of CUEDC2, as demonstrated by inhibition of the generation of MDA and increased activity of SOD and CAT; however, the increase of CAT activity following transfection with siCUE was not significant. The aforementioned results are consistent with a previous study where ablation of CUEDC2 protected cardiomyocytes against oxidative stress by facilitating stability of the antioxidant enzyme glutathione peroxidase 1 (17). Apoptosis can be mediated by DOX-induced oxidative

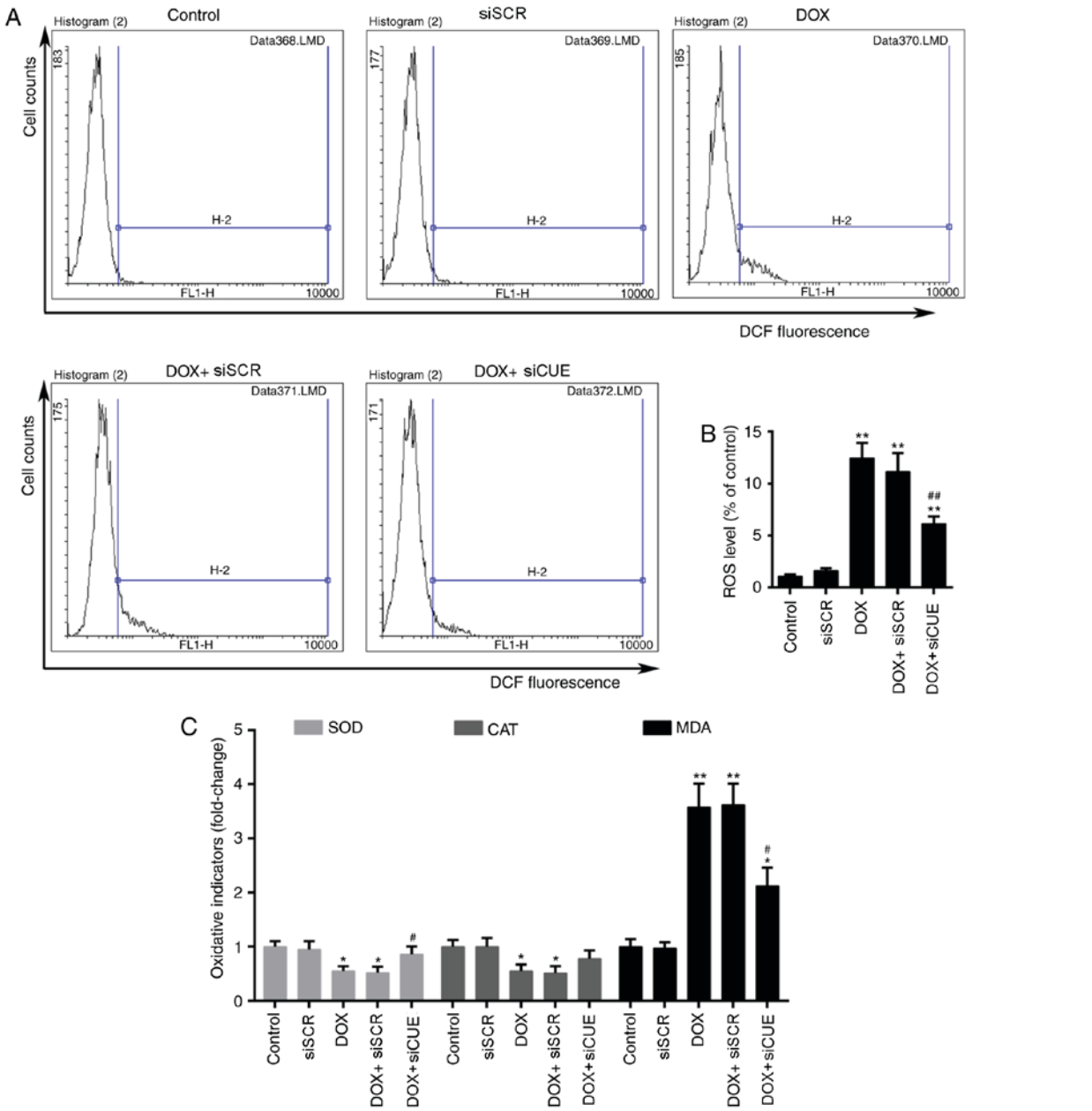

Figure 2. Flow cytometry (A) histograms and (B) quantitative analysis, as used to determine ROS levels. (C) Relative activity of oxidative stress indicators MDA, SOD and CAT. *P<0.05 and **P<0.01 vs. the control group. $^{\#}$P<0.05 and $^{\#\#}$P<0.01 vs. the DOX group. CUEDC2, CUE domain-containing 2; CAT, catalase; DCF, 2',7'-dichlorofluorescein; DOX, doxorubicin; MDA, malondialdehyde; ROS, reactive oxygen species; siCUE, CUEDC2 siRNA; siRNA, small interfering RNA; siSCR, siRNA scramble control; SOD, superoxide dismutase.

stress (30). Loss of MMP has been demonstrated to occur during the early stage of apoptosis (31). In the present study, loss of MMP was effectively recovered by the depletion of CUEDC2, thus indicating that silencing CUEDC2 improved mitochondrial function. Apoptosis rate was decreased by ~50% in the CUEDC2 depletion group compared with in the DOX group. Bcl-2 is an anti-apoptotic protein, whereas Bax is a proapoptotic protein (32,33). Furthermore, diverse apoptosis pathways converge on a mechanism associated with caspase-3 (34,35), and the release of cytochrome *c* from mitochondria to cytosol can act as an intermediate to induce apoptosis (36). The results of the present study revealed that the DOX-induced elevated expression levels of Bax, cleaved caspase-3 and cytochrome *c* were decreased in the CUEDC2 depletion group. Conversely, the decreased expression of Bcl-2 was rescued by depletion of CUEDC2. Taken together, downregulation of CUEDC2 may prevent DOX-induced oxidative stress and apoptosis. FOXO transcription factors are implicated in numerous cellular responses (8). Among the FOXO proteins, FOXO3a has been extensively studied and has been demonstrated to serve a role in the stress response (37-39). It has been reported that phosphorylated AKT, as a mediator of cellular processes, may phosphorylate FOXO3a to inhibit its activity, thereby disrupting transcription of its target genes, including Bim (11). As a target of FOXO3, Bim is also associated with apoptosis caused by stress (40). To further determine the underlying mechanisms of DOX-induced cardiotoxicity, involvement of the

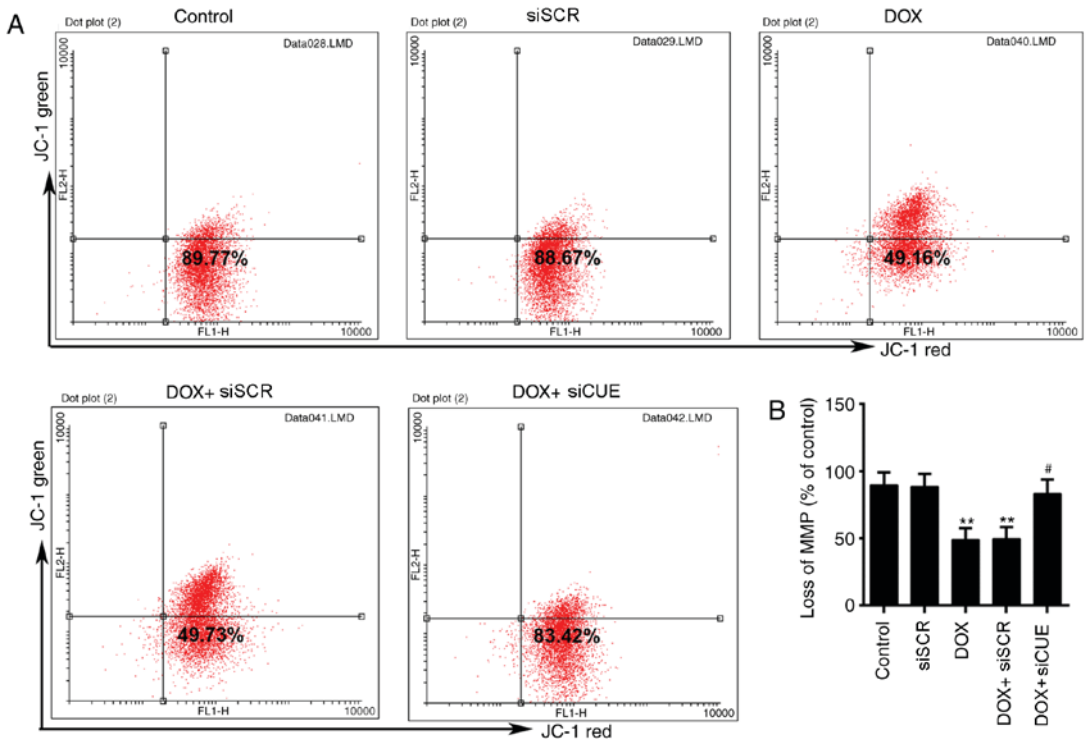

Figure 3. (A) MMP detection by flow cytometry. (B) Determination of MMP loss. **P<0.01 vs. the control group. $^{\#}$P<0.05 vs. the DOX group. DOX, doxorubicin; MMP, mitochondrial membrane potential; siCUE, CUEDC2 siRNA; siRNA, small interfering RNA; siSCR, siRNA scramble control.

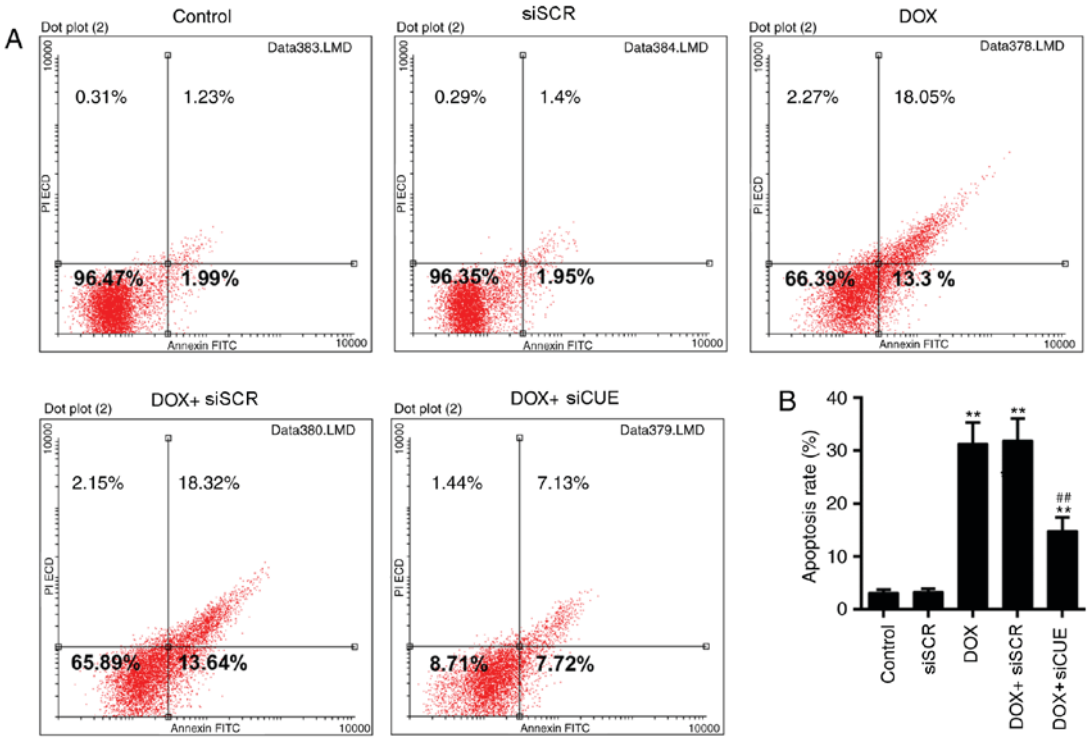

Figure 4. (A) Apoptosis detection by flow cytometry. (B) Determination of apoptosis rate. **P<0.01 vs. the control group. $^{\#\#}$P<0.01 vs. the DOX group. DOX, doxorubicin; FITC, fluorescein isothiocyanate; PI, propidium iodide; siCUE, CUEDC2 siRNA; siRNA, small interfering RNA; siSCR, siRNA scramble control.

AKT/FOXO3a/Bim signaling pathway was examined. The results demonstrated that the expression levels of p-AKT and p-FOXO3a were increased in the CUEDC2 depletion group, whereas Bim expression was downregulated. This suggests that siCUE activated p-AKT, and subsequently the levels of p-FOXO3a and Bim were increased and decreased by p-AKT, respectively. However, this was not fully determined by the present study and thus requires further investigation. In the

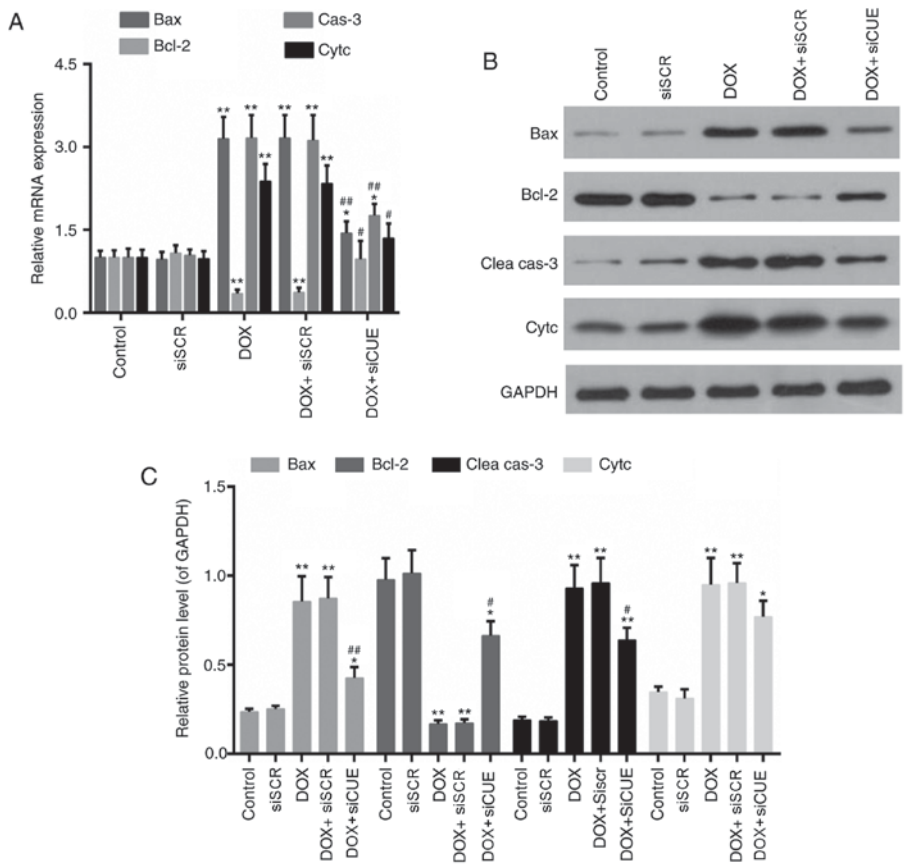

Figure 5. (A) mRNA expression levels of Bax, Bcl-2, cas-3 and Cytc. (B) Western blot and (C) semi-quantitative analysis of the protein expression levels of Bax, Bcl-2, Clea cas-3 and Cytc. GAPDH was used as a loading control. *P<0.05 and **P<0.01 vs. the control group. $^{\#}$P<0.05 and $^{\#\#}$P<0.01 vs. the DOX group. Bax, Bcl-2-associated X protein; Bcl-2, B-cell lymphoma 2; Clea cas-3, cleaved caspase-3; Cytc, cytochrome *c*; DOX, doxorubicin; siCUE, CUEDC2 siRNA; siRNA, small interfering RNA; siSCR, siRNA scramble control.

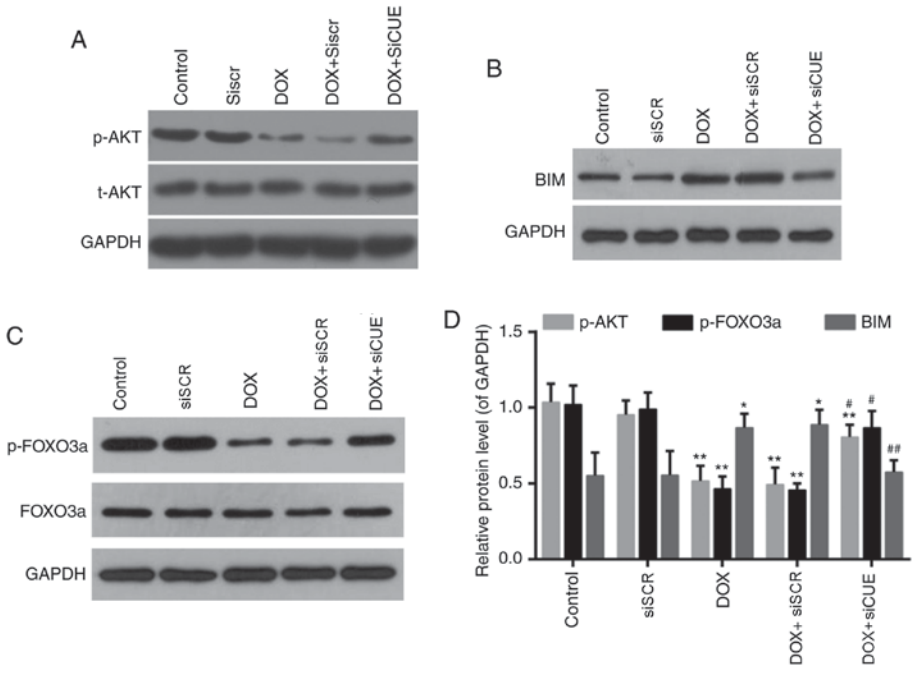

Figure 6. Western blot analysis of (A) p-AKT and AKT, (B) BIM, and (C) p-FOXO3a and FOXO3a. (D) Relative protein expression levels of p-AKT, p-FOXO3a and BIM. GAPDH was used as a loading control. *P<0.05 and **P<0.01 vs. the control group. $^{\#}$P<0.05 and $^{\#\#}$P<0.01 vs. the DOX group. AKT, protein kinase B; BIM, B-cell lymphoma 2-like protein 11; DOX, doxorubicin; FOXO3a, forkhead box O3a; p, phosphorylated; siCUE, CUEDC2 siRNA; siRNA, small interfering RNA; siSCR, siRNA scramble control.

present study, the AKT/FOXO3a/Bim signaling pathway exerted a positive role in the prevention of DOX-induced cardiotoxicity, which was in agreement with the results of a previous study (41). In addition, NAD-dependent protein deacetylase sirtuin-1 has been reported to exhibit synergetic effects on phosphoinositide 3-kinase/AKT that augment the protective effects of exercise on the heart (11). Therefore, it is possible that other signaling pathways may be involved in regulation of FOXO3a. The present study demonstrated that downregulation of CUEDC2 was beneficial and alleviated DOX-induced toxicity in H9c2 cells. The results of the present study are supported by results of a previous study where overexpression of CUEDC2 was considered a predictor of poor prognosis of ovarian serous carcinoma (42). However, a recent study reported that CUEDC2 knockdown could increase tumor growth in lung adenocarcinoma (43). It has therefore been suggested that the function of CUEDC2 may be dependent on cell type. Therefore, it is necessary to perform further in-depth investigations, including *in vivo* animal studies, to elucidate the underlying mechanism of CUEDC2, as CUEDC2 may exhibit different functions *in vitro* and *in vivo*. Taken together, CUEDC2 may be used as a therapeutic target for the treatment of cardiac injury.

In conclusion, the present study demonstrated that downregulation of CUEDC2 prevented DOX-induced cardiotoxicity by alleviating oxidative stress, maintaining MMP and inhibiting apoptosis. It was also demonstrated that the AKT/FOXO3a/Bim signaling pathway serves a role in the cardioprotective mechanism of CUEDC2 knockdown. The results of the present study indicated that modulating the expression of CUEDC2 may be a novel therapeutic strategy to mitigate DOX-associated cardiotoxicity in the future.

Acknowledgements

Not applicable.

Funding

No funding was received.

Availability of data and materials

All data generated and/or analyzed during this study are included in this published article.

Authors' contributions

XZ and WC designed the study. JL, YC, JY and XL performed the experiments. JL and YC performed data analysis. XZ wrote the manuscript. XZ, JL and WC contributed to manuscript revisions.

Ethics approval and consent to participate

Not applicable.

Consent for publication

Not applicable.

Competing interests

The authors declare that they have no competing interests.

References

1. Capranico G, Kohn KW and Pommier Y: Local sequence requirements for DNA cleavage by mammalian topoisomerase II in the presence of doxorubicin. Nucleic Acids Res 18: 6611-6619, 1990.
2. Young RC, Ozols RF and Myers CE: The anthracycline neoplastic drugs. N Engl J Med 305: 139-153, 1981.
3. Thorn CF, Oshiro C, Marsh S, Hernandez-Boussard T, McLeod H, Klein TE and Altman RB: Doxorubicin pathways: Pharmacodynamics and adverse effects. Pharmacogenet Genomics 21: 440-446, 2011.
4. Orhan B: Doxorubicin cardiotoxicity: Growing importance. J Clin Oncol 17: 2294-2296, 1999.
5. Samuel L: Doxorubicin-induced cardiotoxicity. Postgrad Med J 71: 318, 1995.
6. Pereira GC, Pereira SP, Pereira CV, Lumini JA, Magalhães J, Ascensão A, Santos MS, Bjork JA, Moreno AJ, Wallace KB, *et al*: Doxorubicin-induced cardiac, hepatic and renal mitochondrial toxicity in an acute versus sub-chronic treatment model. Biochim Biophys Acta 1797, (Supple): S81, 2010.
7. Skladanowski A and Konopa J: Adriamycin and daunomycin induce programmed cell death (apoptosis) in tumour cells. Biochem Pharmacol 46: 375-382, 1993.
8. Carter ME and Brunet A: FOXO transcription factors. Curr Biol 17: R113-R114, 2007.
9. Li M, Chiu JF, Mossman BT and Fukagawa NK: Down-regulation of manganese-superoxide dismutase through phosphorylation of FOXO3a by Akt in explanted vascular smooth muscle cells from old rats. J Biol Chem 281: 40429-40439, 2006.
10. Yang Y, Zhao Y, Liao W, Yang J, Wu L, Zheng Z, Yu Y, Zhou W, Li L, Feng J, *et al*: Acetylation of FoxO1 activates Bim expression to induce apoptosis in response to histone deacetylase inhibitor depsipeptide treatment. Neoplasia 11: 313-324, 2009.
11. Lin CH, Lin CC, Ting WJ, Pai PY, Kuo CH, Ho TJ, Kuo WW, Chang CH, Huang CY and Lin WT: Resveratrol enhanced FOXO3 phosphorylation via synergetic activation of SIRT1 and PI3K/Akt signaling to improve the effects of exercise in elderly rat hearts. Age (Dordr) 36: 9705, 2014.
12. Sharma G, Kar S, Palit S and Das PK: 18β-glycyrrhetinic acid induces apoptosis through modulation of Akt/FOXO3a/Bim pathway in human breast cancer MCF-7 cells. J Cell Physiol 227: 1923-1931, 2012.
13. Zhang PJ, Zhao J, Li HY, Man JH, He K, Zhou T, Pan X, Li AL, Gong WL, Jin BF, *et al*: CUE domain containing 2 regulates degradation of progesterone receptor by ubiquitin-proteasome. Embo J 26: 1831-1842, 2007.
14. Man J and Zhang X: CUEDC2: An emerging key player in inflammation and tumorigenesis. Protein Cell 2: 699-703, 2011.
15. Livak KJ and Schmittgen TD: Analysis of relative gene expression data using real-time quantitative PCR and the 2(-Delta Delta C(T)) method. Methods 25: 402-408, 2001.
16. Kotamraju S, Konorev EA, Joseph J and Kalyanaraman B: Doxorubicin-induced apoptosis in endothelial cells and cardiomyocytes is ameliorated by nitrone spin traps and ebselen. Role of reactive oxygen and nitrogen species. J Biol Chem 275: 33585-33592, 2000.
17. Jian Z, Liang B, Pan X, Xu G, Guo SS, Li T, Zhou T, Xiao YB and Li AL: CUEDC2 modulates cardiomyocyte oxidative capacity by regulating GPX1 stability. EMBO Mol Med 8: 813-829, 2016.
18. Morakinyo A, Iranloye B and Adegoke O: Calcium antagonists modulate oxidative stress and acrosomal reaction in rat spermatozoa. Arch Med Sci 7: 613-618, 2011.
19. Kalivendi SV, Konorev EA, Cunningham S, Vanamala SK, Kaji EH, Joseph J and Kalyanaraman B: Doxorubicin activates nuclear factor of activated T-lymphocytes and Fas ligand transcription: Role of mitochondrial reactive oxygen species and calcium. Biochem J 389: 527-539, 2005.
20. Konorev EA, Kennedy MC and Kalyanaraman B: Cell-permeable superoxide dismutase and glutathione peroxidase mimetics afford superior protection against doxorubicin-induced cardiotoxicity: The role of reactive oxygen and nitrogen intermediates. Arch Biochem Biophys 368: 421-428, 1999.

21. Gomez-Cabrera MC, Sanchis-Gomar F, Garcia-Valles R, Pareja-Galeano H, Gambini J, Borras C and Vina J: Mitochondria as sources and targets of damage in cellular aging. Clin Chem Lab Med 50: 1287-1295, 2012.
22. Takasaki A, Hanyu H, Iwamoto T, Shirato K, Izumi R, Toyota H, Mizuguchi J, Miyazawa K and Tomoda A: Mitochondrial depolarization and apoptosis associated with sustained activation of c-jun-N-terminal kinasein the human multiple myeloma cell line U266 induced by 2-aminophenoxazine-3-one. Mol Med Rep 2: 199-203, 2009.
23. Luo H, Yang Y, Duan J, Wu P, Jiang Q and Xu C: PTEN-regulated AKT/FoxO3a/Bim signaling contributes to reactive oxygen species-mediated apoptosis in selenite-treated colorectal cancer cells. Cell Death Dis 4: e481, 2013.
24. Xiong H, Wang J, Guan H, Wu J, Xu R, Wang M, Rong X, Huang K, Huang J, Liao Q, *et al*: SphK1 confers resistance to apoptosis in gastric cancer cells by downregulating Bim via stimulating Akt/FoxO3a signaling. Oncol Rep 32: 1369-1373, 2014.
25. Arola OJ, Saraste A, Pulkki K, Kallajoki M, Parvinen M and Voipio-Pulkki LM: Acute doxorubicin cardiotoxicity involves cardiomyocyte apoptosis. Cancer Res 60: 1789-1792, 2000.
26. Kimes BW and Brandt BL: Properties of a clonal muscle cell line from rat heart. Exp Cell Res 98: 367-381, 1976.
27. Hescheler J, Meyer R, Plant S, Krautwurst D, Rosenthal W and Schultz G: Morphological, biochemical, and electrophysiological characterization of a clonal cell (H9c2) line from rat heart. Circ Res 69: 1476-1486, 1991.
28. Sipido KR and Marban E: L-type calcium channels, potassium channels, and novel nonspecific cation channels in a clonal muscle cell line derived from embryonic rat ventricle. Circ Res 69: 1487-1499, 1991.
29. Watkins SJ, Borthwick GM and Arthur HM: The H9C2 cell line and primary neonatal cardiomyocyte cells show similar hypertrophic responses in vitro. In vitro Cell Dev Biol Anim 47: 125-131, 2011.
30. Arstall MA, Sawyer DB, Fukazawa R and Kelly RA: Cytokine-mediated apoptosis in cardiac myocytes: The role of inducible nitric oxide synthase induction and peroxynitrite generation. Circ Res 85: 829-840, 1999.
31. Ly JD, Grubb DR and Lawen A: The mitochondrial membrane potential (deltapsi(m)) in apoptosis; an update. Apoptosis 8: 115-128, 2003.
32. Sharifi AM, Mousavi SH and Jorjani M: Effect of chronic lead exposure on pro-apoptotic Bax and anti-apoptotic Bcl-2 protein expression in rat hippocampus in vivo. Cell Mol Neurobiol 30: 769-774, 2010.
33. Zhai D, Jin C, Huang Z, Satterthwait AC and Reed JC: Differential regulation of Bax and Bak by anti-apoptotic Bcl-2 family proteins Bcl-B and Mcl-1. J Biol Chem 283: 9580-9586, 2008.
34. Salvesen GS: Caspases: Opening the boxes and interpreting the arrows. Cell Death Differ 9: 3-5, 2002.
35. Ghavami S, Hashemi M, Ande SR, Yeganeh B, Xiao W, Eshraghi M, Bus CJ, Kadkhoda K, Wiechec E, Halayko AJ and Los M: Apoptosis and cancer: Mutations within caspase genes. J Med Genet 46: 497-510, 2009.
36. Yang J, Liu X, Bhalla K, Kim CN, Ibrado AM, Cai J, Peng TI, Jones DP and Wang X: Prevention of apoptosis by Bcl-2: Release of cytochrome c from mitochondria blocked. Science 275: 1129-1132, 1997.
37. Lam EW, Francis RE and Petkovic M: FOXO transcription factors: Key regulators of cell fate. Biochem Soc Trans 34: 722-726, 2006.
38. Sunters A, Fernández de Mattos S, Stahl M, Brosens JJ, Zoumpoulidou G, Saunders CA, Coffer PJ, Medema RH, Coombes RC and Lam EW: FoxO3a transcriptional regulation of Bim controls apoptosis in paclitaxel-treated breast cancer cell lines. J Biol Chem 278: 49795-49805, 2003.
39. Sunters A, Madureira PA, Pomeranz KM, Aubert M, Brosens JJ, Cook SJ, Burgering BM, Coombes RC and Lam EW: Paclitaxel-induced nuclear translocation of FOXO3a in breast cancer cells is mediated by c-Jun NH2-terminal kinase and Akt. Cancer Res 66: 212-220, 2006.
40. Concannon CG, Tuffy LP, Weisová P, Bonner HP, Davila D, Bonner C, Devocelle MC, Strasser A, Ward MW and Prehn JH: AMP kinase-mediated activation of the BH3-only protein Bim couples energy depletion to stress-induced apoptosis. J Cell Biol 189: 83-94, 2010.
41. Samuel SM, Thirunavukkarasu M, Penumathsa SV, Paul D and Maulik N: Akt/FOXO3a/SIRT1-mediated cardioprotection by n-tyrosol against ischemic stress in rat in vivo model of myocardial infarction: Switching gears toward survival and longevity. J Agric Food Chem 56: 9692-9698, 2008.
42. Wang A, Guo C, Sun Y, Lu L, Wang Y, Wang Q, Zhang Y, Zhang H, Wang L, Gu Y, *et al*: Overexpression of CUEDC2 predicts poor prognosis in ovarian serous carcinomas. J Cancer 6: 542-547, 2015.
43. Sun L, Bai L, Lin G, Wang R, Liu Y, Cai J, Guo Y, Zhu Z and Xie C: CUEDC2 down-regulation is associated with tumor growth and poor prognosis in lung adenocarcinoma. Oncotarget 6: 20685-20696, 2015.